

Hydraulics of simple habitat structures

Hydraulique des structures d'habitat simples

H. SHAMLOO, *Department of Civil Engineering, K.N.T University of Technology, Tehran, Iran, 19697*

N. RAJARATNAM, *Department of Civil Engineering, University of Alberta, Edmonton, Alberta, Canada, T6G 2G7*

C. KATOPODIS, *Freshwater Institute, Department of Fisheries and Oceans, Winnipeg, Canada, R37 2N4*

ABSTRACT

Habitat structures are built in rivers to provide feeding and resting areas for fish. At the present time, only rough guidelines are available for the design of these structures. This paper presents the results of a laboratory study on the flow and erosion around simple habitat structures. Hemispheres with diameter D of 74 and 130 mm were placed on smooth, rough as well as erodible beds and Froude number of the approaching flow was in the range of 0.074 to 0.6. The relative depth d/h where d is the depth of and h is the height of the body was found to be the important parameter and was varied from about 0.6 to 4.3. Four different regimes of flow were found, which were classified based on the relative depth. Downstream of the body, there was a recirculation region (closed wake) with a length of about $2D$ which was followed by an open turbulent wake. The structure of flow in this open wake was analyzed in two layers using the concept of the wall wake. In the plane of symmetry, the inner layer was analyzed using the law of the wall whereas the outer layer was analyzed using the wake equation of Schlichting. The variation of the velocity in the transverse direction was also analyzed using the concept of similar profiles. Further an empirical correlation was found for the velocity scale. The amplification of the bed shear stress near the body, especially for the rough bed was significant. Some observations were also made on the nature of erosion around the hemisphere placed on erodible beds of two sand sizes of 1.11 and 2.1 mm. It was found that the pattern of erosion was different for the different flow regimes. The maximum equilibrium clear water scour depth occurred in front of hemispherical bodies and was approximately equal to $0.67 D$.

RÉSUMÉ

Des structures d'habitat sont construites en rivières pour fournir des aires de repos et de nourriture aux poissons. Actuellement on ne dispose que de guides approximatifs pour concevoir ces ouvrages. Cet article présente les résultats d'une étude, en laboratoire, de l'écoulement et de l'érosion autour d'ouvrages d'habitat simples. Des hémisphères, de diamètre $D = 74$ et 130 mm, ont été placés sur des lits soit lisses, soit rugueux et également à fond mobile, les nombres de Froude de l'écoulement amont variant entre 0.074 et 0.6. La profondeur relative d/h , où d est la profondeur d'eau et h la hauteur de l'obstacle, s'est révélée être un paramètre important ; elle variait entre 0.6 et 4.3. On a trouvé quatre régimes d'écoulement différents qui ont été classés en fonction de la profondeur relative. À l'aval de l'obstacle se trouvait une zone de recirculation (sillage fermé) de longueur environ $2D$, suivie d'un sillage ouvert turbulent. La structure de l'écoulement dans ce sillage ouvert a été analysée en deux couches, selon le concept du sillage pariétal. Dans le plan de symétrie, la couche interne a été assimilée à une loi de paroi, et la couche externe, à l'équation de sillage de Schlichting. La variation de vitesse dans la direction transversale a été analysée quant à elle, avec le concept des profils auto-semblables. On a établi de plus, une corrélation empirique pour l'échelle de vitesse. L'accroissement de la contrainte au fond près de l'obstacle était significative, surtout dans le cas du lit rugueux. Quelques observations ont été faites également sur la nature de l'érosion autour de l'hémisphère placé sur des fonds mobiles comportant deux tailles de grains de 1.11 et 2.1 mm respectivement. Il s'est avéré que la forme de l'érosion était différente selon les régimes d'écoulements. La profondeur d'affouillement maximum à l'équilibre en eau claire était située en avant des obstacles hémisphériques, et était à peu près égale à $0.67 D$.

Introduction

Fish habitat in rivers, including areas for spawning, feeding, cover and resting, are endangered by the construction of hydraulic structures like dams and weirs and river training works and by channelization. Often measures are taken to offset fish habitat losses or to improve and diversify existing degraded habitat. Such measures include the installation of rocks, rock clusters, rock weirs and other instream works. These are known collectively as fish habitat structures and have been used in Canada and several other countries. Stream and river improvement or restoration projects also use habitat structures in an effort to mimic natural features such as rock clusters, rapids, pools and riffles (Katopodis 1996). At the present time, only rough guidelines exist for the design of such structures (Low 1992). The lack of comprehensive studies of habitat structures has been noted as well as the long term limitations of such approaches (Katopodis 1996; Kellerhals and Miles 1996). Comprehensive hydraulic studies would contribute to better and more effective design of such structures. At-

tractive features of these habitat structures are their downstream wakes with larger depths and smaller velocities, providing cover, resting and feeding opportunities for fish.

Even though wakes have been studied extensively in Fluid Mechanics (see Schlichting 1979; Chang 1970 and Zdravkovich 1997), most of these studies deal with deeply submerged wakes, located away from boundaries. The characteristics of these wakes depend mainly on the Reynolds number, in addition to the body geometry. But in rivers in which these habitat structures are installed, the depth of flow d is generally of the same order as the height h of the structure and the effect of the bed is also important. As a result, the approaching flow is affected by the habitat structure, with significant changes to the water surface. These wakes may also be affected by the Froude number of the approaching flow in addition to the Reynolds number. Our knowledge of these essentially Froudean wakes is very limited and this paper presents the results of a laboratory study on the main characteristics of these wakes, under rather simple conditions including erosion around these structures. Practical use of the results

Revision received September 15, 2000. Open for discussion till February 28, 2002.

presented in this paper would require field experiments with target fishes.

Review of Literature

Flow around an obstacle placed on the bed of a flume shows a family of vortices formed in its wake and front. Investigations on flow around bluff bodies (Okamoto et al. 1977; Okamoto 1980; Baker 1979 and Schwind 1962), for an open-ended obstacle (an obstacle placed on a boundary) in a shear flow, show that two kinds of vortices are produced. These are the horse-shoe vortices (HS vortices), which are generated upstream of the frontal face of the object on the ground (on which the object is mounted) and the arch vortices generated behind the separation line on the body (Fig. 1 (a)). Adverse pressure gradient causes the approaching boundary layer to separate upstream of the obstacle. Part of this separated flow forms the horse-shoe vortices which produce high bed shear stress which in turn could cause erosion around the obstacle.

The general structure of two dimensional wakes can be explained by the dual-wake concept of primary and secondary wakes (Fan and Tsuchiya 1990). The primary wake is the enclosed region immediately behind the body with circulatory flow pattern. The free shear layers leaving the body, bound the primary wake. The velocity outside the wake is approximately equal to the free stream velocity and is smaller inside and hence the free shear layers tend to roll up into discrete vortices. The vortex velocity in the primary wake is constant (Tsuchiya 1987). The secondary wake has an open structure and includes the free shear layers and vortices

from the primary wake in the form of the Karman vortex street and extends far downstream. The results obtained in this study indicate that three dimensional wakes bounded by a boundary could also be described by a similar model.

Okamoto (1979) conducted a series of experiments to investigate the turbulent shear flow behind a hemisphere-cylinder placed on the ground and observed that arch vortices were shed from the body and were gradually pushed downstream by a strong downwash behind the obstacle until they almost touched the ground. Okamoto also found that on the boundary, the pressure was the lowest where the roots of the arch vortices were attached.

Martinuzzi and Tropea (1993) observed up to four HS vortices upstream of the obstacle. It was found that the recirculation region for a three dimensional body is much shorter than that of the two-dimensional case. Results of Logan and Lin (1982) and Fackrell and Pearce (1981) indicated the same conclusions. It was proposed that in the case of a three dimensional body, part of the flow goes around the body whereas for a two dimensional body such as a bridge pier, most of the deflected fluid, flows around of the body, enlarging the recirculation zone. Larousse et al. (1991) found that the two legs of the HS vortex behind a cube downstream of the reattachment point were still present and they remained adjacent to one another, with no further stream-wise vortices occurring in between. The location of the legs further downstream became closer to the axis of symmetry. It was proposed that this is due to the influence of the recirculation vortex which entrained the inner portions of the HS vortex and drew the legs towards the axis of symmetry.

Hunt et al. (1978) showed that the separation regions have fluid passing through them and are the origins of the line vortices that are shed into the downstream flow. Schofield and Logan (1990) investigated the flow around three-dimensional obstacles and confirmed this finding. Fisher and Klingeman (1984) studied local scour near fish habitat structures and found HS-vortices similar to those occurring at piers. Cullen (1991) used four different models of fish rocks in a laboratory flume and found similar patterns. Dwivedi et al. (1992) observed that the recirculation region behind a hemisphere moves to the water surface as the Froude number increases, for the same depth of flow to height of body ratio d/h .

Experimental arrangement and experiments

The experimental work was performed in a tilting flume, 1.22 m wide, 0.65 m deep and 18 m long with a tailgate to control the depth of flow. The discharge was measured with a magnetic flow meter installed in the supply line. Two Styrofoam hemispheres of diameters D of 130 and 74 mm and heights h of 65 and 37 mm were used as obstacles in the flow. These hemispheres were mounted on the smooth aluminum bed. Red food color plumes were used to visualize the flow. Observations were made with flow depths of 32 to 268 mm and discharges up to 68 L/s with the Froude number, F as low as 0.074 for flow visualization and as high as 0.6 for velocity and shear stress measurements. The relative depth d/h was in the range of 0.65 to 4.26. All measurements were carried out in a region of fully developed flow. The ratio of

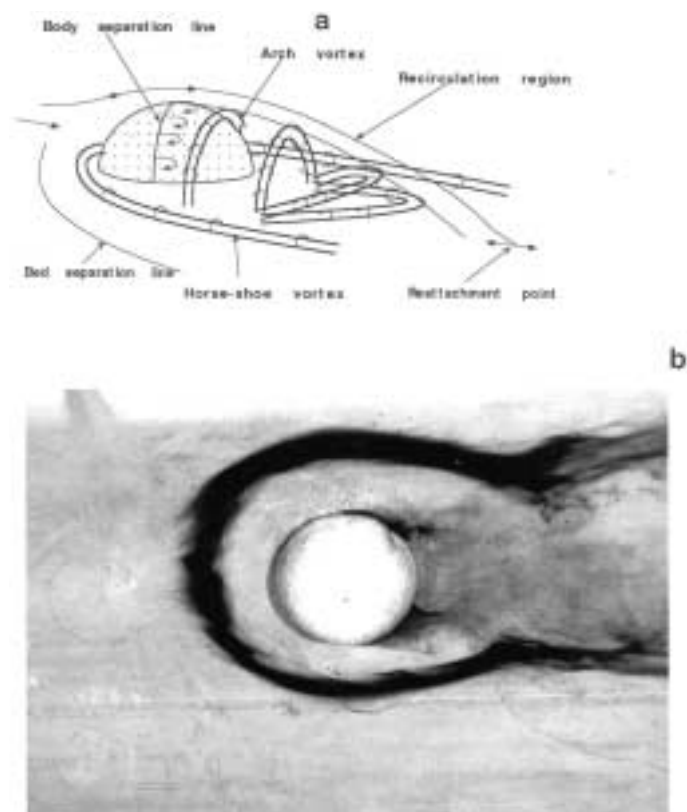


Fig. 1. (a) Vortex systems around the obstacle for regimes 1 and 2. (b) Trace of horse-shoe vortex and separation line on the bed.

width to depth of most of flows was in the range of 9.4 to 16.5 which ensured the existence of one dimensional flow in the central part of the flume where the bodies were placed.

Primary details of the experiments are shown in Table-1. Four series of experiments, referred to as A, B, C and D, were performed. In the A series, the d/h ratio was in the range of 1.26 to 1.89. The corresponding d/h ranges for the B, C and D series were respectively 1.08 to 1.11, 0.62 to 0.69 and 4.12 to 4.26. In Table-1, in the code describing the experiments, the second letter of S, R and M indicates a smooth, rough or mobile bed. The third character indicates the type of obstacle used, with 0 indicating the initial test without any body in the flow, 1 and 2 indicating respectively hemispheres with D=130 and 74 mm. A cube of sides of 74 mm was referred to as 3 with 4 representing a natural rock and both these bodies were used only in the erosion experiments. The fourth character of 1 or 2 indicates the size D_{50} of the essentially uniform sand used in the erosion experiments, equal to 1.1 and 2.1 mm.

In experiments for studying erosion, a false floor, 110 mm high, 1.22 m wide and 10.5 m long was placed on the original aluminum floor and two different sands of D_{50} of 1.1 mm and 2.1 mm were used. The thickness of the sediment layer was 20 mm on the raised floor, with a deeper bed near the obstacles. A wooden board, 0.61 m wide and 1.22 m long, with sand particles glued on it, was placed beneath the body for the experiments with the rough bed. All the erosion experiments were carried out for the

clear-water scour case.

Two-dimensional velocity and bed shear stress measurements were made with yaw and pitch probes (Rajaratnam and Muralidhar 1967), connected to pressure transducers. These probes were used only when the third component of velocity was negligible. The velocity profile method was used for bed shear stress measurements in the flow upstream of the obstacles and the yaw probe was used as a Preston tube in local bed shear measurements around the bodies (Rajaratnam and Muralidhar 1968). The thickness of the large yaw probe was 2.8 mm and that of the smaller one was 1.1 mm. The vertical thickness of the pitch probe was 9.9 mm. Two different commercial Prandtl tubes were used with external diameters of 3 mm and 1.6 mm.

Measurements were carried out in the vertical plane of symmetry (POS), upstream and downstream of the body. Measurements in the lateral directions were also made at different stations downstream of the hemisphere, for different values of y/h where y is the vertical distance above the bed. Based on the magnitude of turbulence present in the flow, the period of each measurement was set. For the Prandtl tube in unidirectional flow, a frequency of 25 Hz was used with a duration of 240 seconds. The frequency for two dimensional velocities was 12.5 Hz with a duration of 200 seconds. In more turbulent flows, the sample number and the duration of the measurements had to be increased to obtain a better average.

The uncertainties in the measurements are estimated using the

Table-1. Primary details of the experiments

Series	No.	D(cm)	h(cm)	Q(L/s)	d(cm)	Uo(m/s)	F	Re	d/h
	AS0			54	12	0.369	0.340	44,262	
	AS1	13	6.5	54	12	0.369	0.340	44,262	1.85
	AS2	7.4	3.7	34	7	0.398	0.480	27,869	1.89
	AR11	13	6.5	40	12	0.273	0.252	32,787	1.85
	AM01			40	12	0.273	0.252	32,787	
A	AM11	13	6.5	40	12	0.273	0.252	32,787	1.85
	AM21	7.4	3.7	20	7	0.234	0.283	16,393	1.89
	AM31	7.4	3.7	20	7	0.234	0.283	16,393	1.89
	AM41	14	9.5	40	12	0.273	0.252	32,787	1.26
	AM02	13		65	12	0.444	0.409	53,279	
	AM12	13	6.5	65	12	0.444	0.409	53,279	1.85
	BS0			30	7.2	0.342	0.406	24,590	
	BS1	13	6.5	30	7.2	0.342	0.406	24,590	1.11
	BR11	13	6.5	20	7	0.234	0.283	16,393	1.08
	BM01			20	7	0.234	0.283	16,393	
B	BM11	13	6.5	20	7	0.234	0.283	16,393	1.08
	BM21	7.4	3.7	13	4	0.266	0.425	10,656	1.08
	BM31	7.4	3.7	13	4	0.266	0.425	10,656	1.08
	BM02	13	6.5	30	7	0.351	0.424	24,590	1.08
	BM12			30	7	0.351	0.424	24,590	
	CS0			8	4.2	0.156	0.243	6,557	
	CS1	13	6.5	8	4.2	0.156	0.243	6,557	0.65
	CR11	13	6.5	13	4	0.266	0.425	10,656	0.62
C	CM01			13	4	0.266	0.425	10,656	
	CM11	13	6.5	13	4	0.266	0.425	10,656	0.62
	CM02			20	4.5	0.364	0.548	16,393	
	CM12	13	6.5	20	4.5	0.364	0.548	16,393	0.69
	DS0			70	39.3	0.146	0.074	57,377	
D	DS1	13	6.5	68	26.8	0.208	0.128	55,738	4.12
	DS2	7.4	3.7	65	15.8	0.337	0.271	53,279	4.27

method of Kline and McClintock (1953). The confidence level for all estimates was chosen to be 95%. Geometry of the flume and the dimensions of the obstacles were measured with an uncertainty of ± 0.5 mm. The uncertainty in the measurement of the depth of flow and discharge were found to be respectively ± 1.12 mm and ± 0.5 L/s. The uncertainty in the calculation of the velocities obtained with the pitot-static probe was 12% for the smallest velocity of 0.1 m/s, which reduced to 0.8% for 0.4 m/s. The overall uncertainty was less than the estimated value due to the averaging of a large number of samples. The small yaw and pitch probes were as accurate as the pitot-static probe for smaller yaw and pitch angles ($<15^\circ$).

Vortex systems and general flow patterns

The general flow patterns around the body such as the vortex system, wake and separation points on the bed in front of the obstacle and on the body itself, were studied using dye plumes. Observations were made for Froude number $F=0.004$ to 0.214 and Reynolds number R (based on the depth of flow) in the range of 3000 to 44,000. To locate the regions of high shear stress around the obstacle, dye plumes were introduced close to the bed up-

stream of the obstacle. Due to the presence of adverse pressure gradient in front of the hemisphere, the flow stopped before the separation line and the dye remained on the bed leaving a red line indicating the location of the separation line (Fig. 1(b)). A part of the separated boundary layer formed a HS vortex of large circulation in front of the body which produced high shear stress on the bed. This high shear stress was able to remove the dye sticking to the bed and produced a dye-free zone. Due to the oscillation of the HS vortex, the cleared region was much wider than the actual width of the HS vortex itself. The effect and presence of the HS vortex could be observed over a distance of 2 to 3 D downstream of the body. Separated flow from the sides of the body and the two legs of the HS vortex combined with each other in the wake of the hemisphere. Observation from the sides of the obstacle showed that the height of the HS vortex was about 0.2 h .

As a result of the rotation of the primary HS vortex, a series of smaller vortices was generated. The rotation of the primary HS vortex was clockwise. Every clockwise rotating vortex produced a weak counter clockwise rotating vortex close to the bed. There was a tiny vortex between the primary vortex and the front of the body. It was possible to observe up to four vortices. Baker (1979, 1980) and Martinuzzi and Tropea (1993) also observed up to four HS vortices.

When the relative depth d/h was greater than one, separation of flow from the top and the sides of the obstacle produced an arch-vortex. The arch-vortex behaves like a half-vortex-ring and was observed by dye injection at the sides and top of the obstacle. Significant growth of the shear layer after separation from the body can be attributed to the pairing of vortices. These arch vortices are attached to the bed in the low pressure areas behind the hemisphere.

Effect of Free Surface

The water surface profiles observed for the different experiments are classified into four regimes as shown schematically in Fig.2 (a) with some typical profiles shown in Fig.2 (b). For the relative depth d/h larger than one, the flow passing from the top of the body divided into an upper and lower layer. The lower layer, under the influence of the free shear layer mixes with the wake region while the top layer, depending upon d/h , would not mix with the recirculation zone. Flow with the relative depth greater than about 4 may be classified to be in regime 1. In regime 1 the effect of the body is not felt at the surface and the top layer of the flow does not mix with the wake region.

For the relative depth in the range of 1.3 to 4, the upper layer did not mix with the wake region but surface waves appeared and this is referred to as regime 2 (Fig. 2(c)). In regime 2, the surface flow is in the downstream direction. In regime 2, mixing in the lower layer is shown in Fig. 2 (c) and similar mixing occurred in regime 1 also. But if the relative depth of flow is in the range of 1.1 to 1.3, the free shear layer causes mixing through the whole depth of the flow and some backward flow could be observed near the water surface and this defines regime 3 (Fig.2 (d)). Regime 4 occurs when the relative depth is smaller than 1 and the top of the obstacle is above the water surface and the Karman vortex street

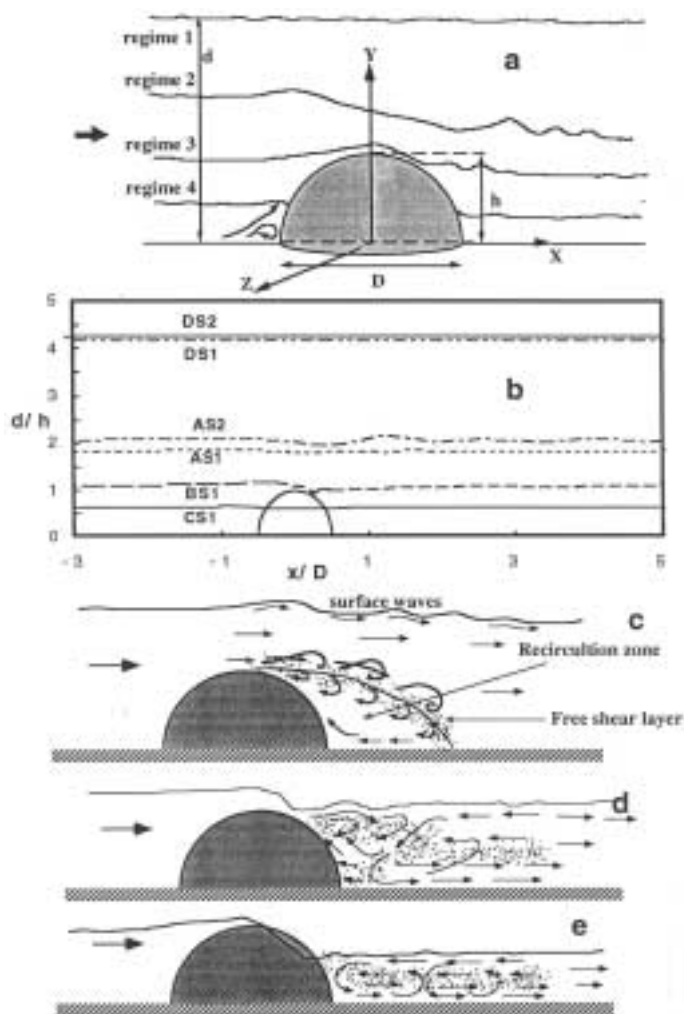


Fig. 2. (a) Definition sketch of different flow regimes (b) Water surface profiles for different regimes (c-e) Details of flow for regimes 2, 3 and 4.

is present with a strong backward flow behind the body (Fig.2 (e)).

In regime 1, flows of relative depths of 4.12 and 4.26 and $F = 0.128$ and 0.272 respectively were studied (see Table-1). The upper layer of the forward flow behaves as a potential flow with no local change in the free surface water profile and no surface waves, whereas in the lower layer, the flow adjacent to the body, separated from the obstacle as form of arch-vortices and created a free shear layer. The vortex system around the obstacle in a fully submerged flow is shown in Fig.1(a) where the arch vortices shed from the body cover the whole recirculation region. Inside the recirculation zone, the flow is backward towards the body and was very turbulent.

In regime 2, a number of cases were studied, with the relative depth in the range of 1.89 to 1.46 and Froude number in the range of 0.34 to 0.562. For a relative depth of 1.85 and F of 0.34, there was a series of 3 surface waves across the width of the flume. The sides of these waves became distorted by the oncoming flow as they were carried downstream and there were not visible for x/D greater than about 3 where x is the longitudinal distance from the center of the body. With a higher F of 0.48 and a relative depth of 1.89, the number of surface waves increased to 7 with larger heights. The length of the recirculation zone was less than $1D$ and it was attached to the bed with a strong backward flow adjacent to the bed. Other investigations have suggested a similar trend. Cantwell and Coles (1983) found the length of the wake to be roughly 1.0 to 1.5 D . Okamoto (1979) also found that due to the presence of a strong downwash behind the sphere, the recirculation region was shortened and limited to 2.5 D and proposed that the reattachment of the outer streamline enclosing the recirculation region could be found by the location of the highest pressure on the ground plane.

In regime 3, the relative depth of the observed flows was in the range of 1.11 to 1.32 and the Froude number ranged from 0.294 to 0.481. The separated flow from the top of the obstacle joined with the separated flow from the sides thereby forming a strong

arch vortex. For a relative depth of 1.32 and $F=0.362$, there were 2 strong waves immediately downstream of the body with short wave length. The presence of a very fast current at the central portion of the surface waves was more significant and the water surface became very rough. The surface waves started to interact with the highly turbulent recirculation zone due to the decrease in the thickness of the top layer. The dye injected on the surface waves could be seen mixing with the recirculation zone. Some backward flow could be observed downstream of these waves at the surface. For most experiments in this regime, the height of the backward flow in the wake behind the body can be divided into two layers, a top layer of backward flow and a lower layer. The top layer of the backward flow after hitting the body in a clockwise rotation moved upward to the surface and joined the separated flow from the top and the surface waves. The lower layer of the backward flow in the recirculation zone dived down after hitting the body in a counter clockwise movement and was swept by the forward flow from the sides. It then created a forward flow downstream of the body near the bed.

In regime 4, when the relative depth is less than about one, the downwash over the body disappears and the wake becomes two-dimensional with the appearance of the Karman vortex street and the disappearance of the arch vortices (Fig.2 (e)). For relative depth of about 0.96 and Froude number in the range of 0.384 and 0.6, the top of the obstacle protruded above the flow and the length of the backward flow region at the surface was about 1.5 D . This backward flow proceeded towards the body, impinged on it and reversed its direction near the bed.

Velocity profiles in the plane of symmetry and in the wake

In this section, typical velocity profiles in the plane of symmetry are presented. Profiles of the longitudinal time averaged velocity u in terms of the mean velocity U_0 of the approach flow are shown in Fig. 3 (a-d), for different values of the relative distance x/D , for four typical experiments for the four regimes. These pro-

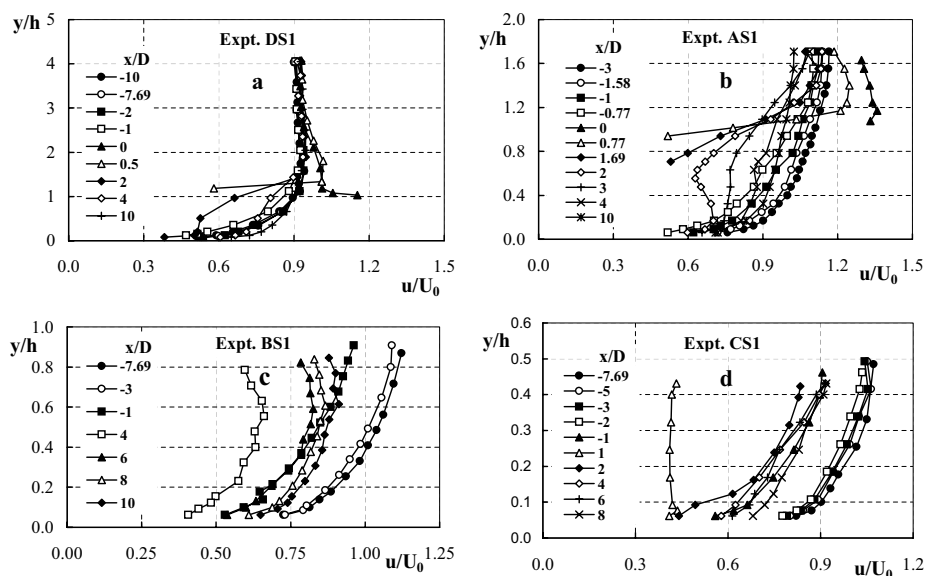


Fig. 3. (a-d) Profile of normalized u velocity for the four regimes.

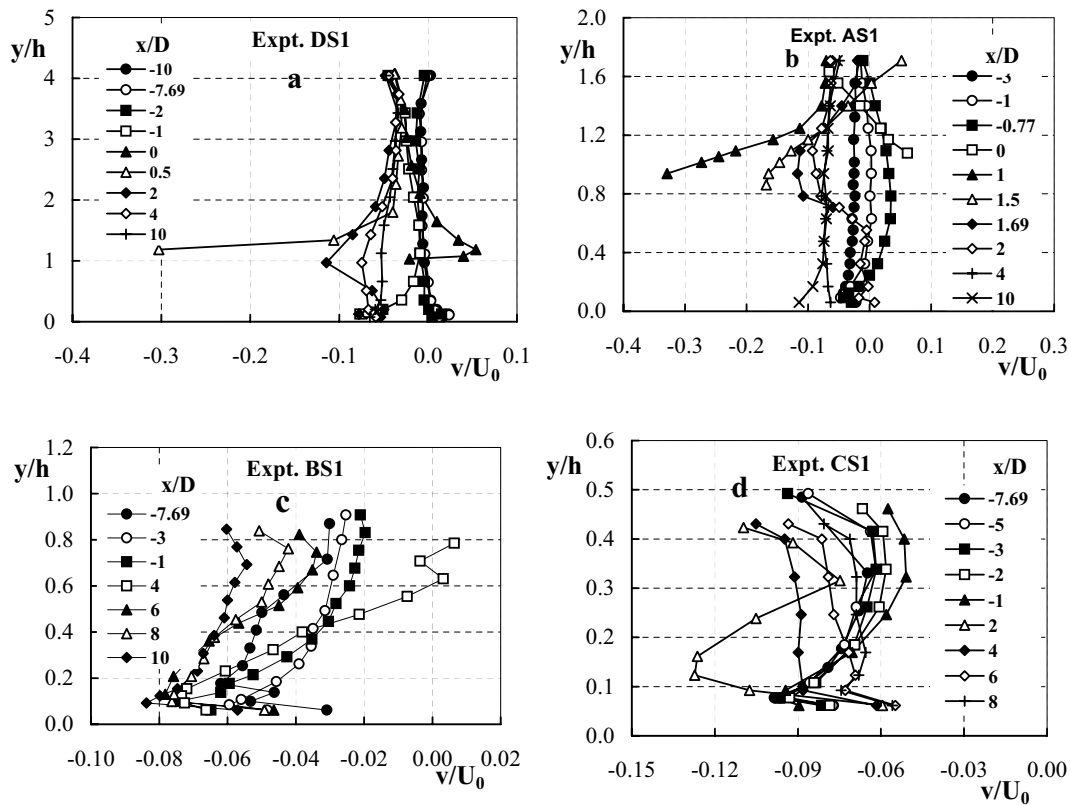


Fig. 4. (a-d) Profile of normalized v velocity for the four regimes.

files show the deceleration of the flow approaching the body, the speeding over the body and eventual approach to the original state far downstream of the body. The upper part of the velocity profile for Expt. DS1 (regime 1) is deformed very much like in potential flow. The retardation of the velocity becomes more significant in regimes 3 and 4 with smaller relative depths. The velocity profiles immediately downstream of the recirculation region are very similar to that of the wall wake profile for relative depths larger than one. Further downstream, the profiles tend to approach their upstream form. The profiles of the vertical velocity v in terms of U_0 are shown in Fig. 4(a-d), wherein dividing flows are termed negative. While the vertical velocities for upstream profiles away from the body are close to zero, near the body ($x/D=-0.77$), the lifting of the velocity vector can be noticed, at least for regimes 1 and 2. In regimes 3 and 4, for the whole depth, the flow dives down due to the effect of the body with its maximum of $v/U_0=-0.1$ with angle of pitch of -9 degrees at $y/h=0.1$, almost twice as that in regimes 1 and 2.

The variation of u/u_* with the dimensionless distance from the bed y_*v/u_* where u_* is the shear velocity at the bed and v is the kinematic viscosity of the fluid, are shown in Fig.5 (a-d) for several values of x/D for four typical experiments. Far upstream from the body, these profiles were found to follow the Prandtl-Karman equation but as the body is approached, these profiles deviate from it. Further, the nature of this deviation appears to be different for each regime. The largest deviations occur immediately upstream and downstream of the body. Similar results for rough beds are shown in Fig. 5(e-f).

Typical transverse profiles of the u velocity are shown in Fig. 6(a-

d) for the section with $x=2D$ (regimes 1 and 2); $x=4D$ (regime 3) and $x=5D$ (regime 4) at different distances above the bed, where z is the transverse distance from the vertical centerplane of the flume and the body. Measured velocity at each level is normalized by average undisturbed velocity of that level itself, U_y . The width of inner wake in regimes 1 and 2 is roughly equal to the diameter of the body while its counterpart in regimes 3 and 4 is almost twice the diameter of the body, indicating a significant increase of width of the wake for the lower relative depths. The presence of the HS vortex can be guessed from the humps present in profiles closer to the body and the bed where the location of the HS vortex was also found by flow visualization. The HS vortex appears to increase the width of the wake.

Fig. 7(a-d) show typical transverse profiles at the level of $y/h=0.5$ for the regimes 1 to 3 and $y/h=0.2$ for regime 4, for several sections with x/D varying from 1.5 to 10. The profiles at these levels are selected as typical of the wake at each station. A significant recovery of the velocity occurs in the central region of the wake in a short distance of less than $10D$. The magnitude of velocity increases rapidly from $z/D=0$ to $z/D=0.5$, in regimes 1 and 2 and more slowly to $z/D=1.2$ in regimes 3 and 4 indicating a larger wake in these regimes. The small hump in the profiles due to the HS vortex is also present up to $x/D=3$ to 4, indicating that HS vortex has lost its identity further downstream and become part of the wake, confirming the results of S. Okamoto (1979). In regimes 3 and 4, velocity recovery continues even as far as $x/D=20$. But in regimes 1 and 2, the velocity in the central region of the wake is larger than the rest of the wake after $x/D=4-6$, due to the downwash of the flow, indicating presence of two peaks in defect

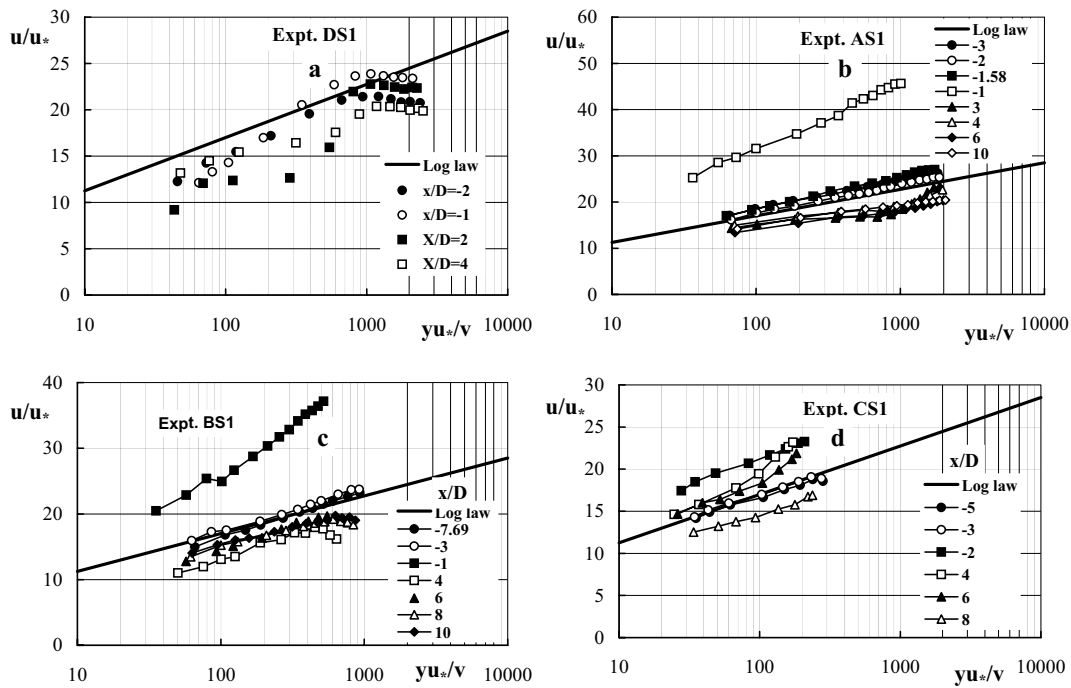


Fig. 5. (a-g) Distribution of u velocity for the four regimes in the Law of the wall form for smooth and rough beds.

velocity distribution which is also reported by other researchers as a ‘negative wake effect’ (Okamoto and Yagita, 1973).

Bed Shear Stress

Bed shear stress τ is important since it is related to scour and transport of sediment. The bed shear stress τ_0 in the approach flow has been used to normalize the bed shear stress and the results for the centerplane are presented in Fig. 8(a-d) for a few typical experiments. Similar variation in the transverse direction for several values of z/D are shown in Fig. 8(e-f) for two experiments. A study of these results show that as the flow approaches the body, the shear stress decreases to zero on the centerplane and remains negative up to the nose of the body. The region of negative shear stress in the wake can also be noticed. Further, the transverse profiles show significant amplifications at the sides of the body. Corresponding results for rough beds are shown in Fig. 9(a-f) wherein amplifications of almost 20 may be seen, indicating potential sites for start of erosion at the sides of the body.

Analysis of flow in the wake

The evolution of the velocity profile in the POS from fully developed flow on the upstream side to the wall-wake profile on the downstream side is shown in Fig. 10(a). The effect of the downwash flow can be seen on the spanwise velocity profiles downstream of the body. In the region immediately downstream of the recirculation zone, one-peak velocity profiles are present which change to two-peak velocity profiles further downstream. The wall-wake (Fig.10(b)) is analyzed using the plane turbulent wall wake model of Rajaratnam and Rai (1979). The velocity profiles on the plane of symmetry downstream of the body in re-

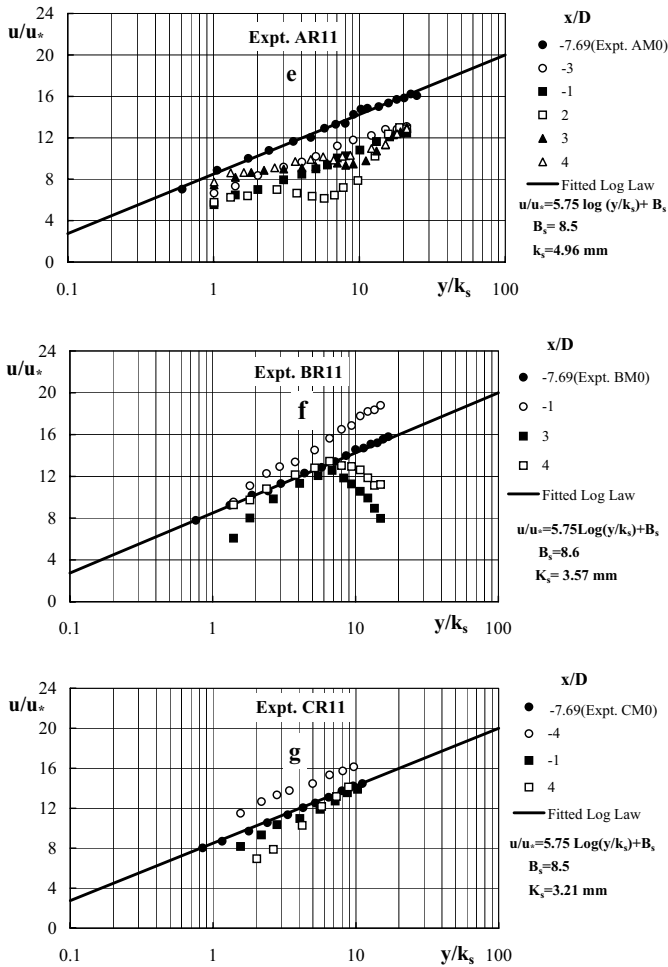


Fig. 5. (a-g) Distribution of u velocity for the four regimes in the Law of the wall form for smooth and rough beds.

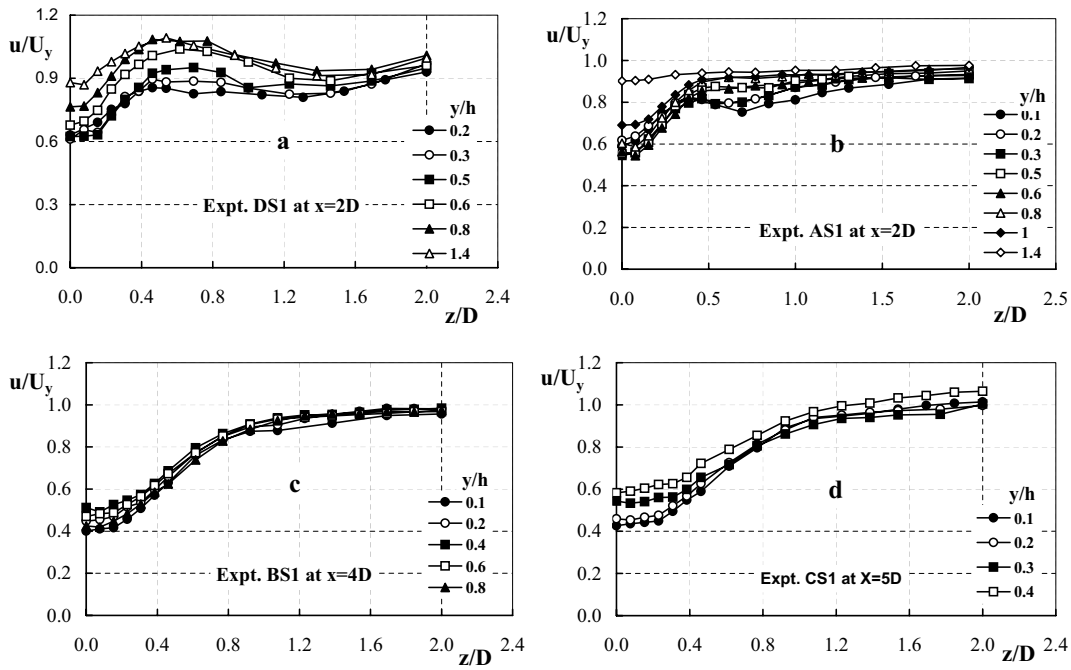


Fig. 6. (a-d) Transverse profiles of u velocity in the wake at $x=2D$ at different distances from bed for the four regimes.

gimes 1 and 2 may be analyzed together where there is a significant thickness of the fluid covering the body. The effect of the bed on the velocity profile is negligible away from the bed in the outer region, whereas close to the bed, its effect is dominant in the inner-region. For the outer region of the wall-wake, the equation of the defect velocity which has been derived for a plane turbulent wake obtained by Schlichting (1930) can be used:

$$\frac{U_0 - u}{u_{1m}} = \left(1 - 0.293 \lambda^{3/2}\right)^2 \quad (1)$$

where u_{1m} is the maximum defect at the center wake (see Fig. 10(b)) and $\lambda=y/b$ where b is the value of y where $u=0.5 u_{1m}$. The maximum velocity at the edge of the outer region was approxi-

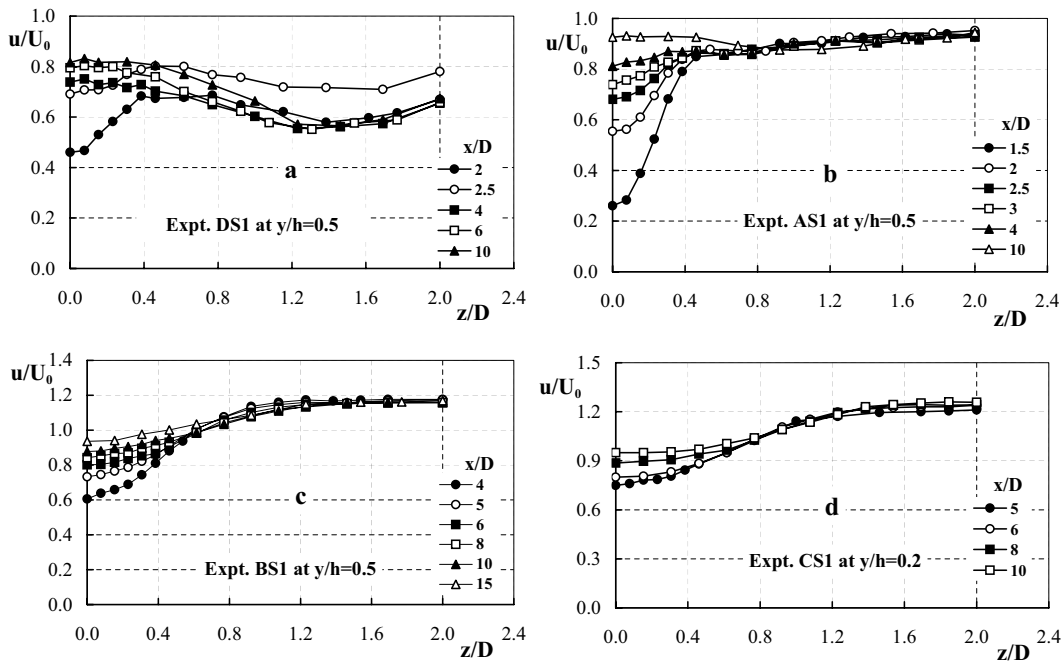


Fig. 7. (a-d) Transverse profiles of u velocity in the wake at $y=0.5h$ at different longitudinal distances for the four regimes.

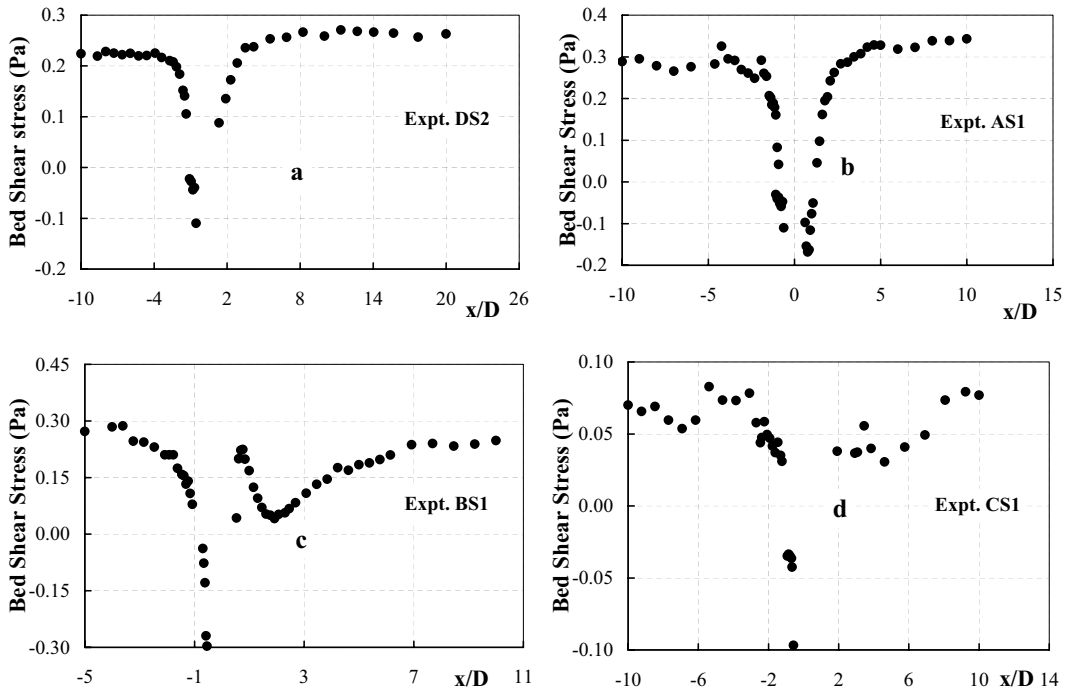


Fig. 8. (a-f) Variation of the bed shear stress in the longitudinal and transverse directions for the smooth bed for the different regimes.

mately equal to the average velocity U_0 and hence is used in place of the maximum velocity in the wake analysis. The parameters u_{1m} and b were obtained using the measured velocity profile and Schlichting's equation. Typical normalized distributions for regimes 1 and 2 are shown in Fig. 11 (a-b) where the distributions

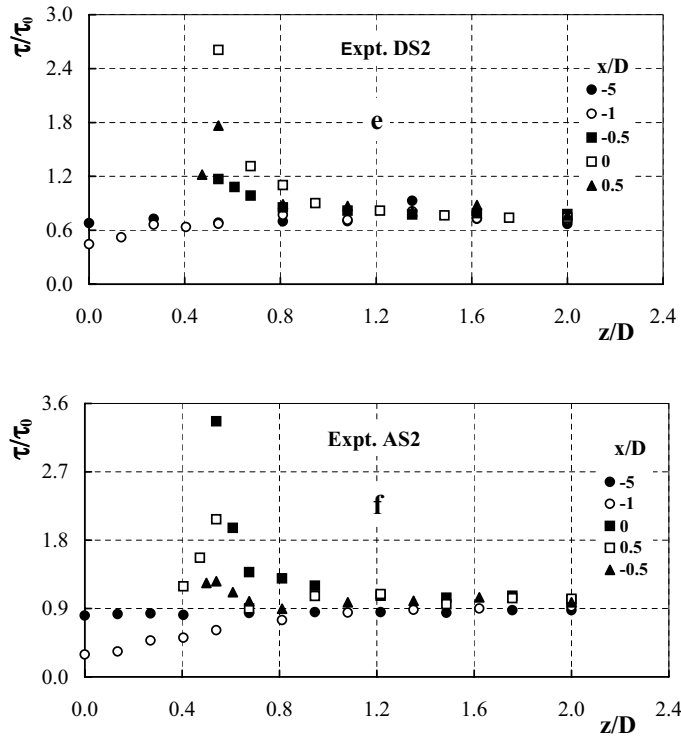


Fig. 8. (a-f) Variation of the bed shear stress in the longitudinal and transverse directions for the smooth bed for the different regimes.

are approximately similar even for relatively small values of x/D . The deviation from plane-wake profile starts at about $y/b=0.5$, close to the bed. The length in which the velocity profiles attain similarity is less than that in the plane-wake for which this transition distance is $12.5D$, which might be attributed to the 3-D effects and presence of the downwash. In the inner region, the velocity profiles were analyzed using the law of the wall and Fig. 12(a-b) show that the law of the wall describes the velocity profiles well. Profiles closer to the body such as x/D of 3 are more prone to deviation from the similarity profile because of possibly the effects of the vortices.

To describe the development of the wake, let us consider the velocity profiles in the wake at a distance of $0.5h$ from the bed. Fig. 13(a-c) show the normalized transverse distribution of the velocity profiles in the wake for the plane with $y=0.5h$, wherein the velocity U_{2D} at $z=2D$ has been used as the velocity scale, for regimes 2, 3 and 4. It is interesting to see that the velocity observations are well described by the plane wake equation. The results of similarity analysis at different depths at $x=2, 4$ and $5D$ are shown in Fig. 14(a-d). Fig. 14 (a-d) show that at small distances ($x=2D$), there are considerable variations from the similarity profile.

Fig. 15 shows the variation of the normalized maximum velocity defect u_{1m}/U_0 with x/D for all the experiments along with the empirical equation suggested by Okamoto for a hemisphere-cylinder placed on the ground floor of a wind tunnel. The results for the present study are described approximately by the equation

$$\frac{u_{1m}}{U_0} = 0.778 \left(\frac{x}{D} \right)^{-0.792} \quad (2)$$

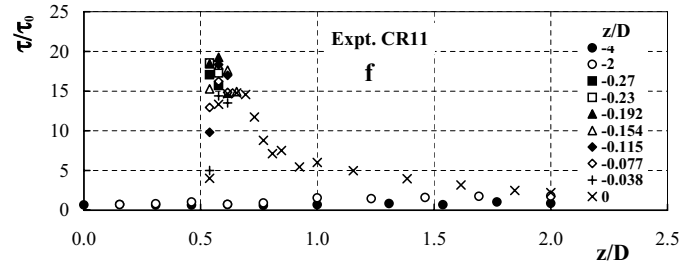
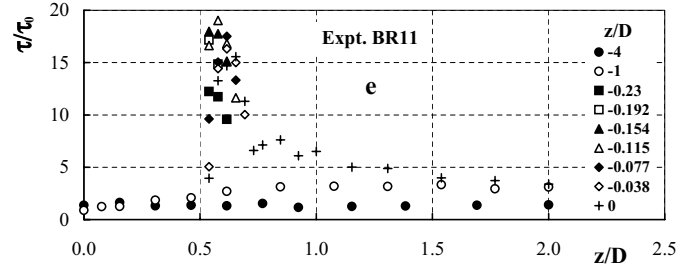
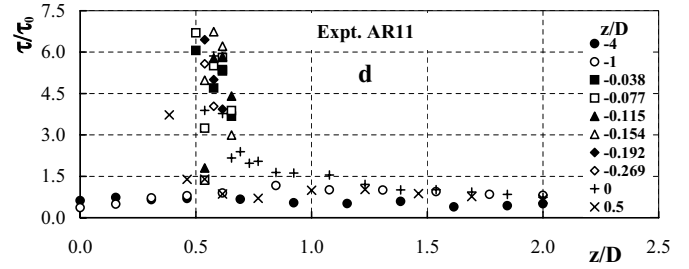
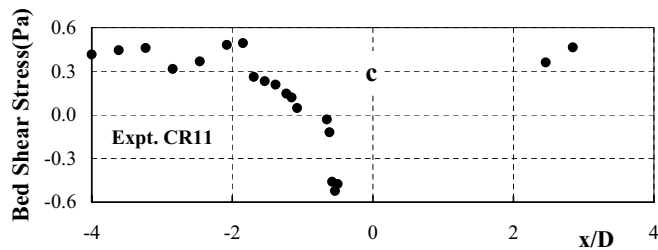
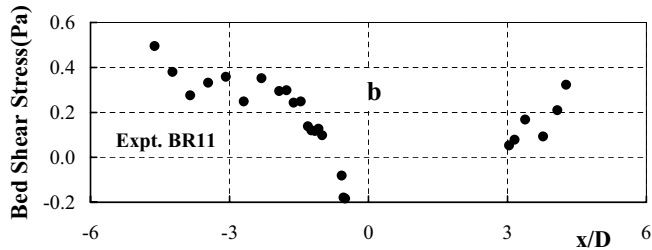
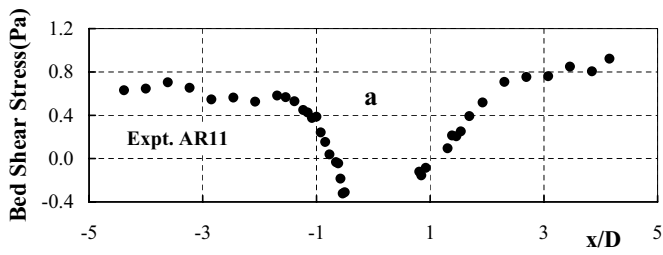


Fig. 9. (a-f) Variation of the bed shear stress in the longitudinal and transverse directions for the rough bed for the different regimes.

Erosion near habitat structures: Experiments and results

Very few investigations (Fisher and Klingeman 1984; Cullen 1991) have been carried out on erosion near habitat structures.

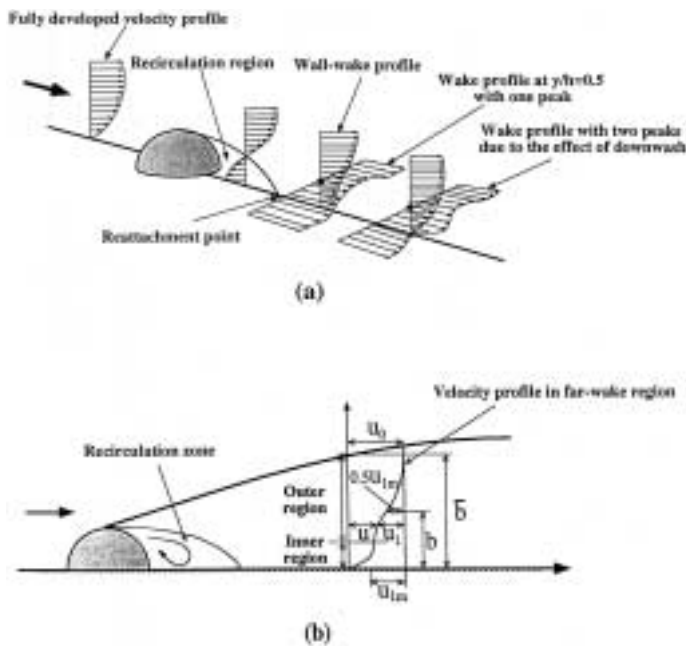


Fig. 10. (a-b) Definition sketches for the velocity field and the wall wake.

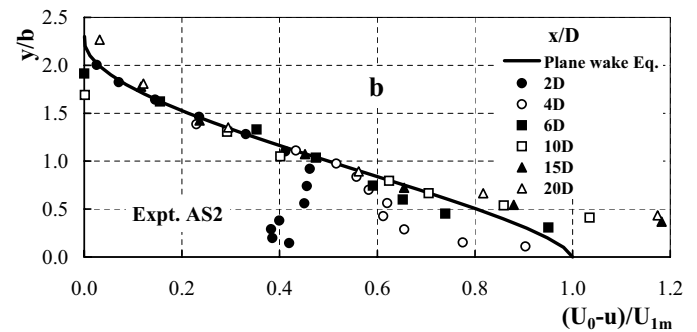
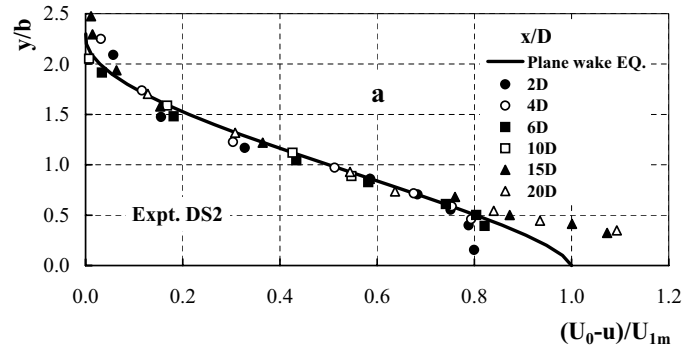


Fig. 11. (a-b) Similarity of velocity profiles in the wake in the POS in the outer region for regimes 1 and 2.

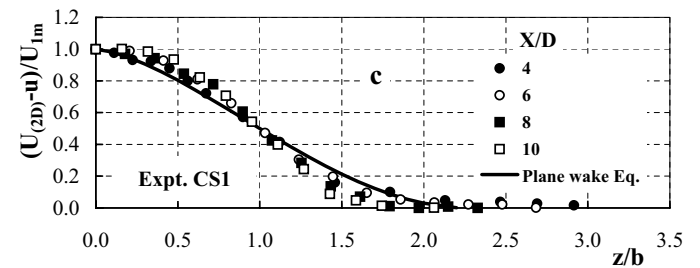
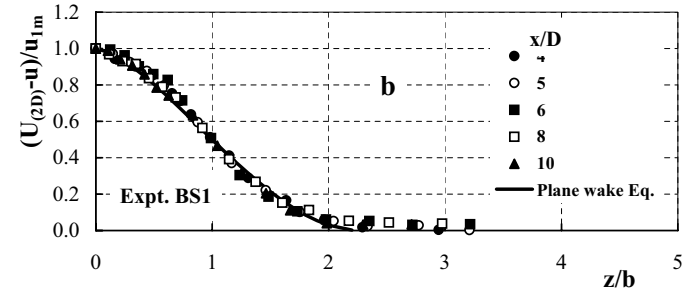
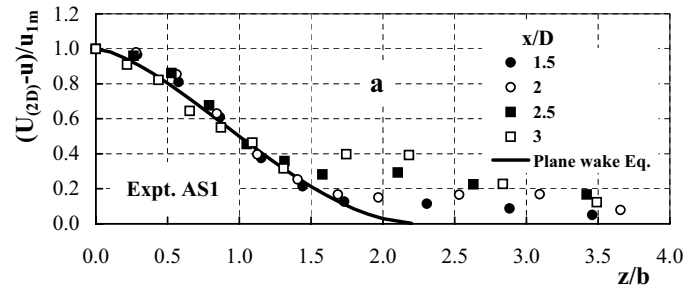
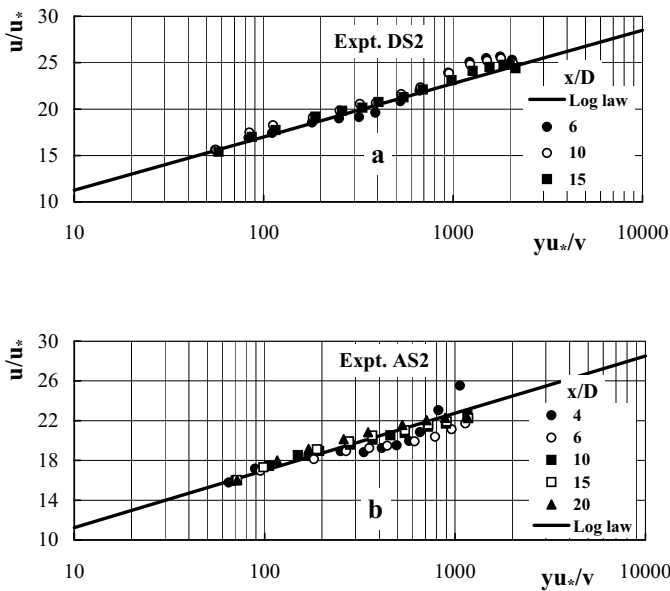


Fig. 12. (a-b) Similarity of velocity profiles in the wake in the POS in the inner region for regimes 1 and 2.

Fisher and Klingeman (1984) carried out a series of experiments in a rectangular flume, 4.9m long, 1.1m wide and 0.5m deep and studied local scour around fish rocks. Coarse sand ($D_{50} = 1.5$ mm) was used as the bed material. It was observed that as the scour depth increased with time at the upstream face of a rock, the rock settled and shifted slightly upstream and settled partly into the scour hole. The depth of scour upstream of the rock increased with depth of water to a maximum value and then decreased as depth of water continued to increase. Maximum ratio of the scour volume to the rock volume occurred at the ratio of water depth to height of rock of about 0.5. In this study eleven series of experiments were performed which

Fig. 13. (a-b) Similarity of transverse velocity profiles in the wake at different distances above the bed for regimes 1 and 2.

included three each for regimes 2 and 3 and two for regime 4 for the hemispherical bodies and the rest for the cube and rock, as

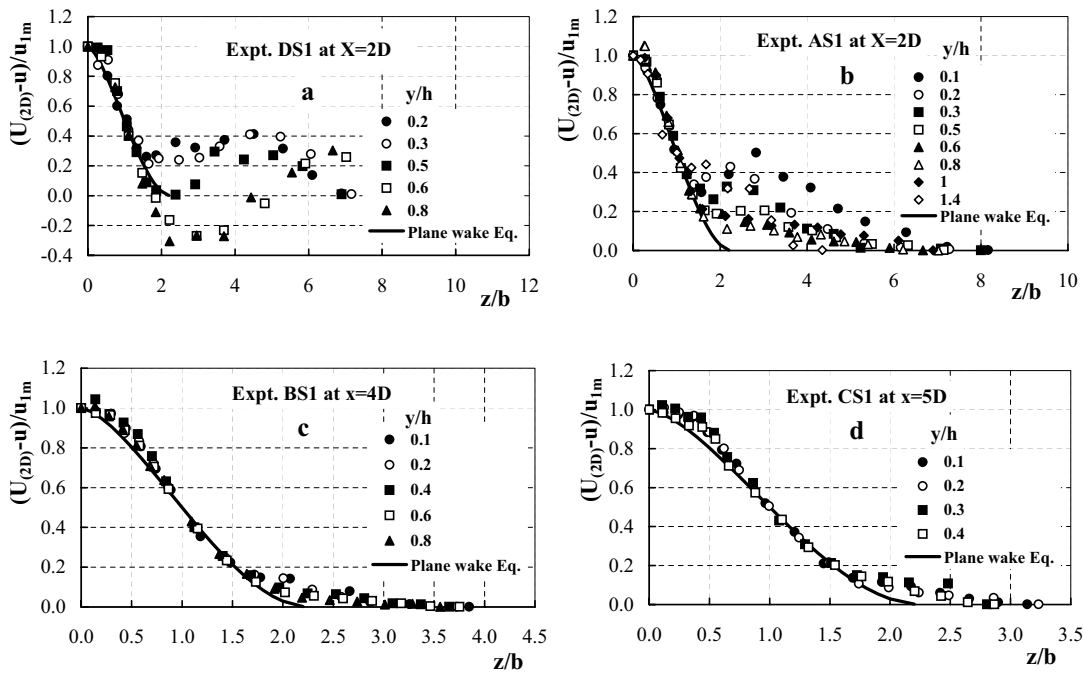


Fig. 14. (a-b) Similarity of transverse velocity profiles in the wake at $y=0.5 h$ for different longitudinal distances for regimes 3 and 4.

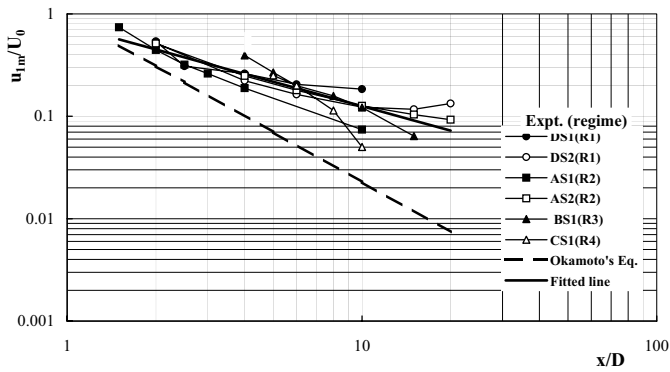


Fig. 15. Decay of the peak velocity defect in the wake with x/D for all the regimes.

indicated in Table-1. These experiments were run until an approximate end or equilibrium state was reached. The scour profile was measured along the POS upstream and downstream of the body and also at its side, at different times, up to about 68 hours. Even though, there was some scouring after the final time of measurement, it is believed that the last profile measured in each experiment is close to the end or equilibrium state.

Typical bed profiles in the front of the body, at its side and at the back for different times and several experiments are shown in Fig. 16(a-i) at different times whereas Fig. 17(a-h) show the end state scour profiles for several experiments, where ϵ is the depth of scour and Δ is the height of deposition at any location. The end state bed profiles in the front of the body have a slope somewhat larger than the angle of repose due to the presence of the horse

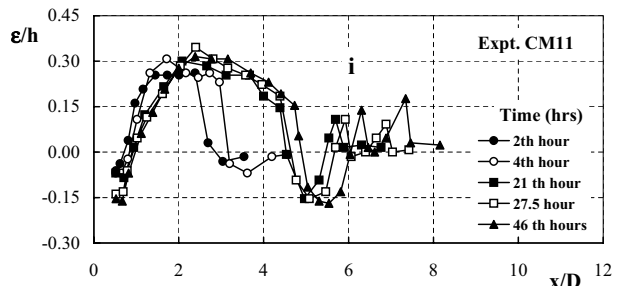
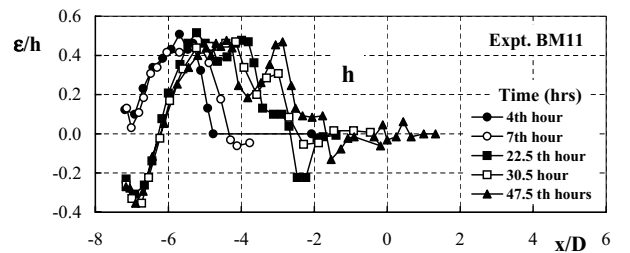
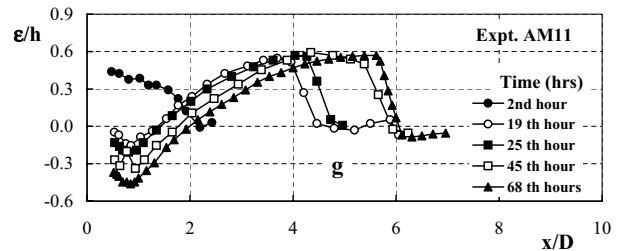
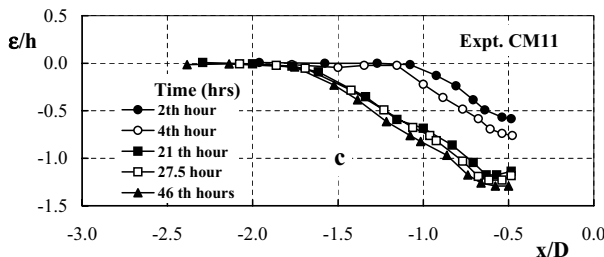
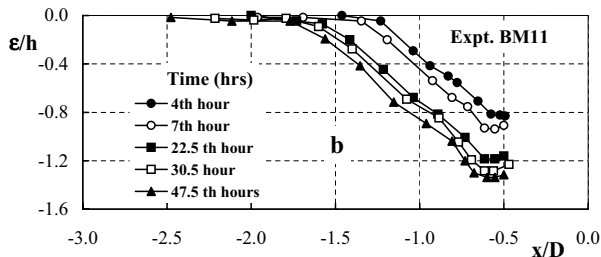
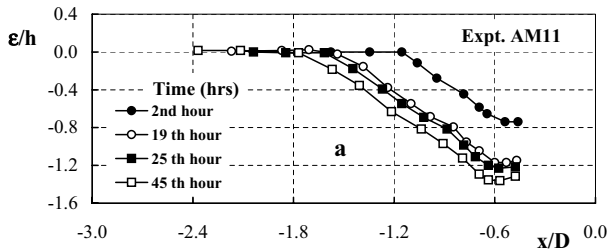
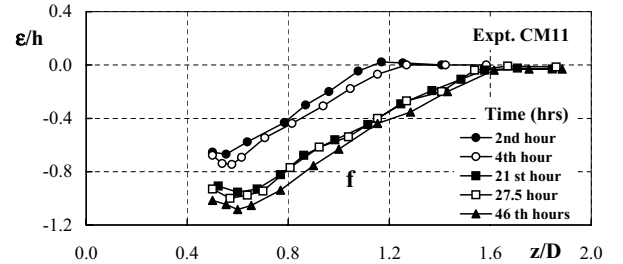
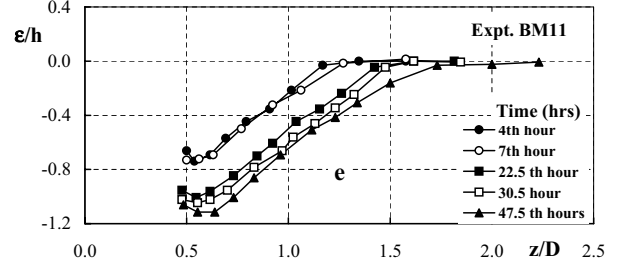
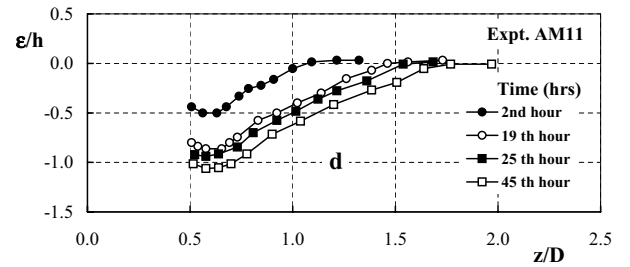


Fig. 16. (a-i) Typical profiles of the eroded bed in the front, side and back of the obstacle at different times for regimes 2 to 4.

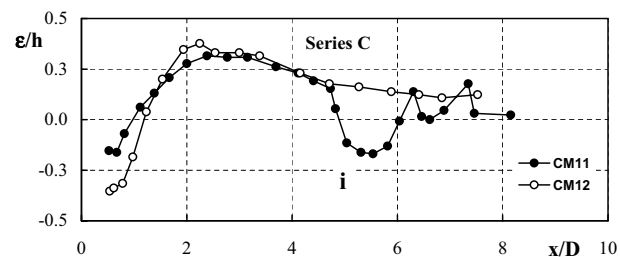
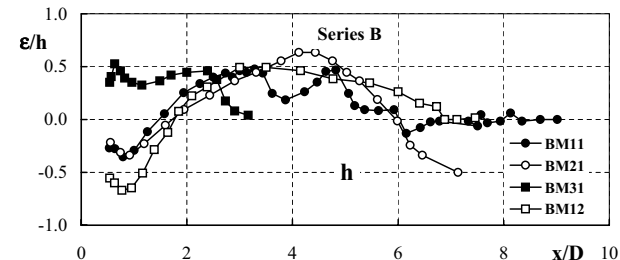
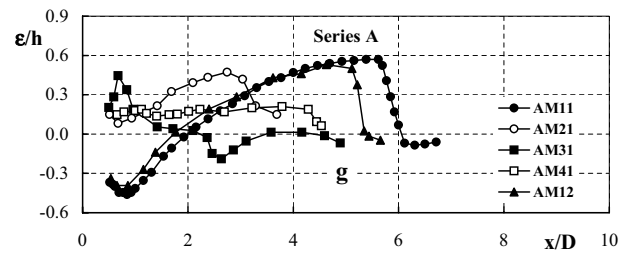
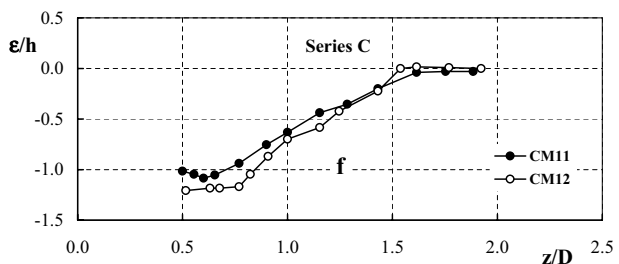
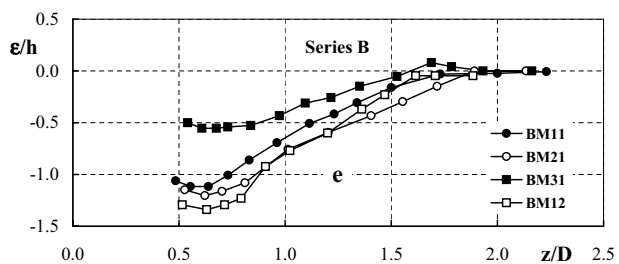
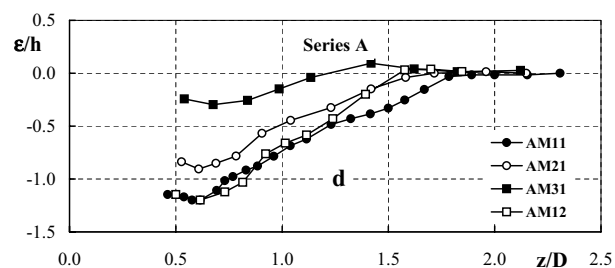
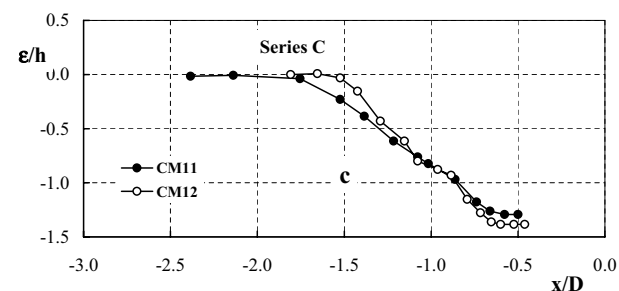
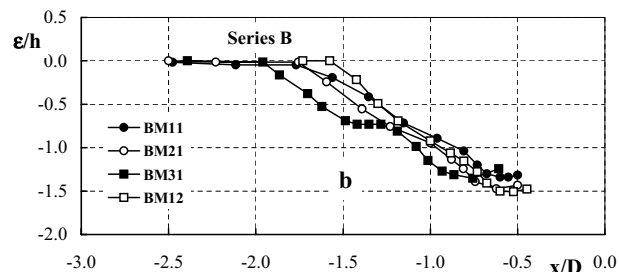
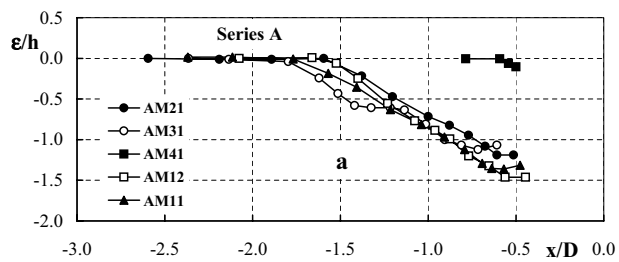


Fig. 17. (a-i) Equilibrium profiles of the eroded bed in the front, side and back of the obstacle for several experiments for regimes 2 to 4.

shoe vortex. The normalized width and depth of the scour holes were almost the same for the different relative depths, suggesting only minor effect of the relative depth on the front scour. Similar comments may also be made on the characteristics of the scour on the side of the bodies. The profiles of the bed at the back of the body in regime 2 show the progress of the profiles over time with an almost constant height, 0.6 h, and parallel slopes.

In an attempt to observe the difference between scour patterns of a simple hemisphere and a cube or a natural rock, scour profiles were measured for the same flow condition for the three bodies. The depth of scour at the side for the cubic obstacle was much smaller than that for the hemisphere (AM11 and AM12). At the back, the scour pattern of the cubic body is different from the hemisphere with a deposition immediately downstream of the body, and then a scour hole. In case of the hemisphere, the two legs of the HS vortex meet each other at the back of the body and create a scour hole there. But the sharp edges of the cube and its flat shape at the back keep the two legs apart and create deposition there. The scour for the natural rock is very small compared with that of other obstacles. The profiles of the scour holes, the end state as well as in the developing stages, were found to be similar, when normalized with suitable length scales of these profiles (Shamloo 1997). The maximum scour depth for the hemispherical bodies was found to be about 0.67 D.

It was found that the pattern of scour and deposition was different for the different regimes and Fig. 18 (a-b) show typical patterns for the regimes 2 and 3. The scour first occurred at the sides of the body and then propagated upstream. The fast spinning of the HS vortex caused the sand particles to be lifted from the bed. On leaving the high velocity region, the sediment particles from the

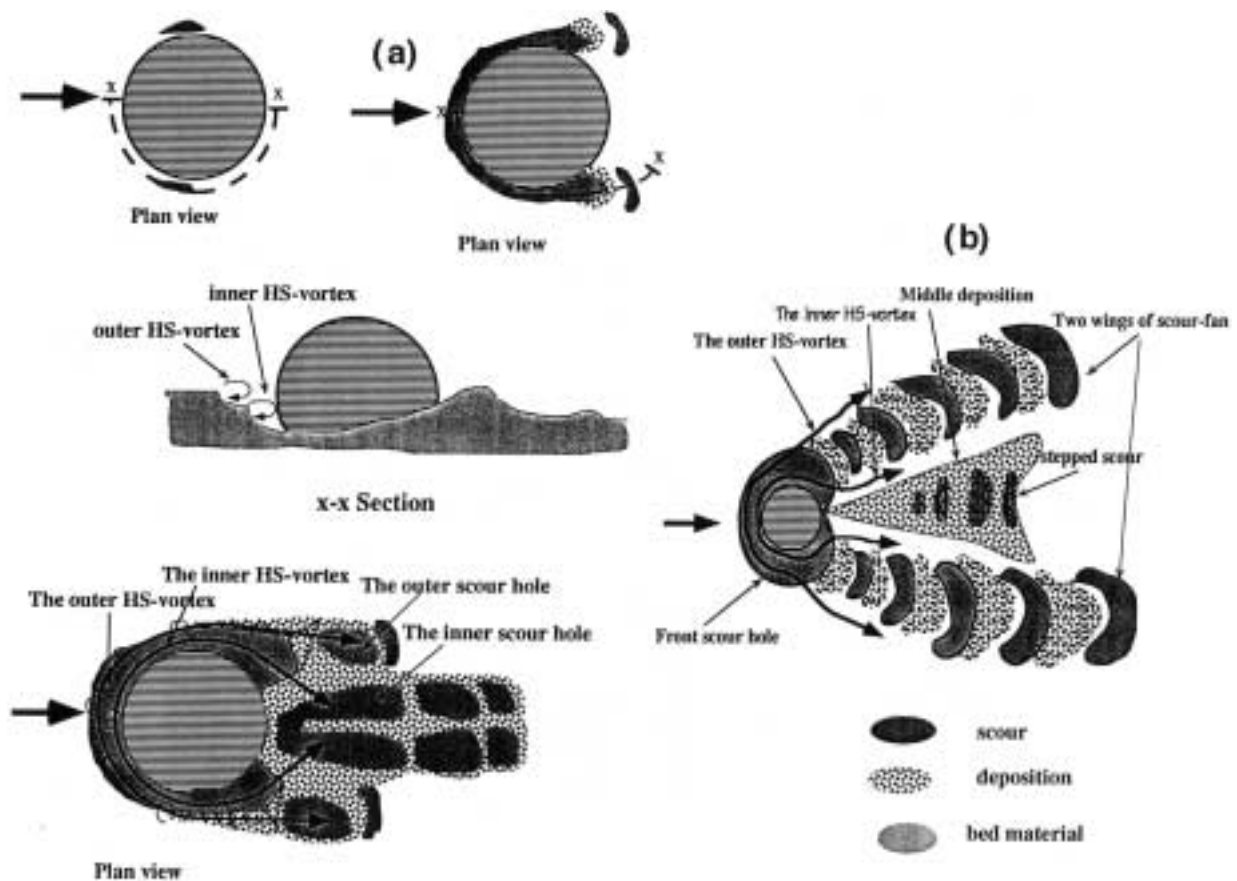


Fig. 18. (a-b) Typical patterns of erosion and deposition for regimes 2 and 3. the different regimes.

scour hole were deposited immediately downstream of the scour hole. The growth of the scour hole around the body caused a stronger down flow at the upstream side of the body which in turn, helped the HS vortex to spin faster, resulting in a deeper scour hole. Due to the effect of this downflow, the scour hole divided into two distinct regions. First was a deeper scour hole adjacent to the body with a steeper slope of the bed at its upstream side. Second was a wider and shallower region with a flatter slope at the upstream side of the first scour hole. These two stages of slopes generated a wider scour hole.

Due to the difference in the strength of the outgoing HS vortices from the scour hole, the resulting deposition hills were formed differently. The stronger vortex was closer to the body and left the body with a smaller angle and a larger deposition closer to the longitudinal axis of the flume and a large and deep scour hole afterward. The outer vortex caused a wider angle and a smaller deposition and scour hole.

There was a distinct difference between the scour patterns of regimes 1 and 2 and regimes 3 and 4. The pattern of scour and deposition in regimes 1 and 2 propagated downstream at the middle with a constant width, but the side scour patterns did not. In regimes 3 and 4, in the absence of the downwash, the side scour patterns propagated while the middle one could not, creating a scour fan with two wings expanding to the sides. The wings of scour patterns were wider and deeper and expanded more in regime 4 than those in regime 3 due to the total absence of the downwash in regime 4.

Conclusions

This paper presents the results of a laboratory study on the sub-critical flow and erosion around simple habitat structures in rivers which are used for the restoration of fish habitat. Hemispheres with diameters of 74 and 130 mm were placed on smooth, rough as well as erodible beds and the Froude number of the approaching flow was in the range of 0.07 to 0.6. The relative depth d/h where d is the depth of the flow and h is the height of the body was found to be the important parameter. Four different regimes of flow were found, which were classified based on the relative depth. Flows with the relative depth greater than 4 fall into regime 1. In regime 1 the effect of the body is not felt at the surface and the top layer of the flow does not mix with the wake. The vortex system around the body consisted of a HS vortex and an arch-vortices. The relative depth in the range of 1.3 to 4 defines regime 2 which was somewhat similar to regime 1 but surface waves started to appear. In regime 3 with d/h in the range of 1 to 1.3, the free shear layer from the body causes the mixing through the whole depth of flow. In this case, some backward flow was present at the water surface. Regime 4 occurs when the relative depth is less than 1; the top of the obstacle is above the water surface and Karman vortex street is present with a strong backward flow behind the body and the arch-vortex system was absent. The wake geometry, the velocity field, bed shear stress and scour patterns were different for the different regimes. Downstream of

the body, there was a recirculation region (closed wake) with a length of about $2D$ which was followed by an open turbulent wake. The structure of flow in this open wake was analyzed using the concept of wall wakes with inner and outer layers. In the plane of symmetry, the inner layer was analyzed using the law of the wall whereas the outer layer was analyzed using the wake equation of Schlichting. The variation of the velocity in the transverse direction was also analyzed using the concept of similar profiles. Further an empirical correlation was found for the velocity scale. The amplification of the bed shear stress near the body, especially for the rough bed, was significant.

Further, some observations were also made on the nature of the erosion around the hemisphere on sand bed for two sizes of 1.11 and 2.1 mm. It was found that the pattern of erosion was different for the different flow regimes. The maximum equilibrium clear water scour depth occurred in front of the body and was approximately equal to $0.67 D$.

It is realized that the results presented in this paper constitute perhaps the first systematic study of the hydraulics of habitat structures in rivers. This study is indeed of a preliminary nature and uses simple bodies. Further studies should be performed with more realistic geometries and should include clusters of rocks and the laboratory results should be supplemented with relevant field observations with target fishes.

Acknowledgment

The work presented in this paper was performed by first author with the supervision of the second and third authors, in the T. Blench Hydraulics Laboratory at the University of Alberta. The authors are thankful to S. Lovell for his help in the experimental work. The first author is also thankful to the Govt. of Islamic Republic of Iran for financial support. Financial support for this study was provided by the Federal Department of Fisheries and Oceans.

Notation

b	length scale for velocity profiles in the wake
b	thickness of the wake
D	diameter of hemispherical obstacle
d	depth of the approaching flow
F	Froude number of the approaching flow
g	acceleration due to gravity
h	height of the obstacle
Q	discharge
R	Reynolds number of the approaching flow
U_0	mean velocity of the approaching flow
U_{2D}	velocity at $z = 2D$
u	time averaged longitudinal velocity component
u_1	velocity defect at any point
u_{1m}	maximum value of the velocity defect
v	time averaged vertical velocity component
x	longitudinal distance measured from the center of the obstacle
y	vertical distance from the bed

z	transverse distance from the centerplane of the flume and the body
Δ	height of deposition at any location
ϵ	depth of erosion at any location
λ	normalized transverse distance in the wake
ρ	mass density of water
ν	kinematic viscosity of water
τ	bed shear stress
τ_0	bed shear stress in the approaching flow

References

- AHMED, F. (1994). Flow and erosion around bridge piers. Ph.D. Thesis, Department of Civil Engineering, University of Alberta, Edmonton, Canada.
- BAKER, C. J. (1979). The laminar horse-shoe vortex. *J. Fluid Mech.*, Vol. 95, part 2, 347-367.
- BAKER, C. J. (1980). The turbulent horse-shoe vortex. *J. of Wind Engrg. and Industrial Aerodynamics*, Vol. 6, pp. 9-23.
- BREUSERS, H.N.C. and A.J. RAUDKIVI (1991). Scouring. IAHR Hydraulic structures Design Manual (2), Balkema Publishers, The Netherlands.
- CHANG, P.K. 1970. Separation of Flow. Pergamon Press, New York, USA, 777 p.
- CULLEN, R.T. (1991). Vortex mechanisms of local scour at model fish rocks. American Fisheries Society Symposium, Vol.10, pp. 213-218.
- DWIVEDI, V.K., N.RAJARATNAM, and KATOPODIS, C. (1993). An exploratory study of fish habitat structures in rivers. Proc. 11th Canadian Hydrotechnical Conference, pp. 573-581.
- FAN, L. S and TSUCHIYA, K. (1990). Bubble Wake Dynamics in Liquids and Liquid- Solid Suspensions. Butterworth and Heinemann, Toronto, 363 p.
- FISHER, A.C., and P.C. KLINGEMAN (1984). Local scour at fish rocks. Water for Resource Development, Proc. ASCE Conf., Coeur d'Alene, USA, pp. 286-290.
- HUNT, J.C.R., C. J. ABELL, J.A. PETERKA, and H.WOO (1978). Kinematical studies of the flows around free or surface-mounted obstacles. *J.Fluid Mech.* Vol. 86, pp.179-200.
- KATOPODIS, C. (1996). Ecohydraulics: challenges and opportunities with fish and fish habitat. Ecohydraulics 2000, Second International Symposium on Habitat Hydraulics, Quebec, Canada, Vol. B, pp 555-578.
- KELLERHALS, R and MILES, M. (1996). Fluvial geomorphology and fish habitat: implications for river restoration. Ecohydraulics 2000, Second International Symposium on Habitat Hydraulics, Quebec, Canada, Vol. A, pp 261-279.
- LAROUSSE, A. R., MARTINUZZI, and C. TROPEA (1991). Flow around surface-mounted, three-dimensional obstacles. Turbulent Shear flows (8), Eighth Int. Symp. on Turbulent Shear Floes, Munich, Germany, SpringerVerlag.
- LOWE, S. (1992). Fish habitat enhancement designs-Typical structures. Alberta Environmental Protection, Edmonton, Alberta, Canada, 32 p.
- MARTINUZZI, R. and C. TROPEA (1993). The flow around surface mounted, prismatic obstacle placed in a fully developed

- channel flow. *J. of Fluids Engineering, ASME*, Vol.115, pp. 85-92.
- OKAMOTO, T., YAGITA, M. (1973). The experimental investigation on the flow past a circular cylinder of finite length. *Bull. Japan Soc. Mech. Eng.* Vol.16, pp. 805-814.
- OKAMOTO, S. (1980), Turbulent shear flow behind a sphere placed on a plane boundary. *Turbulent Shear Flows 2*, Ed. by L.J.S. Bradbury, F. Durst, B.E. Launder, F.W. Schmidt, and J.H. Whitelaw, Springer, Berlin, pp.246-256.
- OKAMOTO, S. (1979). Turbulent shear flow behind hemisphere-cylinder placed on ground plane. *Turbulent Shear Flows 2*, ed. by L.J.S. Bradbury, F. Durst, B.E. Launder, F.W. Schmidt, and J.H. Whitelaw, Springer, New York, pp 171-185.
- OKAMOTO, T., M. YAGITA and S. KATAOKA (1977). Flow past cone placed on flat plate. *Bull. Japan Soc. Mech. Eng.* Vol. 20, pp.329-336.
- RAJARATNAM, N., and MURALIDHAR, D. (1967). Yaw and pitch probes. Tech. Report, Dept. of Civil Engrg., Univ. of Alberta, Edmonton, Canada.
- RAJARATNAM, N., and MURALIDHAR, D. (1968). Yaw probe used as Preston tube. *J. Royal Aero. Soc.*, Vol. 72, pp 1059-1060.
- RAJARATNAM, N and RAI, S. P. (1979). Plane turbulent wall wakes. *ASCE, J of Engrg. Mech.*, Vol. 105, pp. 779-794.
- SCHLICHTING, H. 1979. *Boundary-layer Theory*. McGraw-Hill Book Company, 817p.
- SCHWIND, R. (1962).The three-dimensioal boundary layer near a strut. *Gas Turbine Lab. Rep.*, MIT, USA.
- SCOFIELD, W.H. and E. LOGAN (1990). Turbulent shear flow over surface mounted obstacles. *ASME J of Fluids Engrg.*, Vol. 112, pp. 376-385.
- SHAMLOO, H. (1997). *Hydraulics of simple habitat structures*. PhD Thesis, University of Alberta, Edmonton, Canada, 342p.
- TSUCHIYA, K. (1987). *Wake Dynamics behind a Single Gas Bubble in a liquid andLiquid-Solid Fluidized Media* . Ph.D. Dissertation, Ohio State Univ., Columbus, USA.
- TSUCHIYA, K and L.S. FAN (1986). Near-wake structure of a single gas bubble in a two-dimensioal liquid-solid fluidized bed: Vortex shedding and wake size variation, *Chem. Eng. Sci.* Vol. 43, pp.1167-1181.
- ZDRAVKOVICH, M. M (1997). *Flow Around Circular Cylinders*, Vol.1: *Fundamentals*. Oxford University Press, New York, USA, 672 p.